

Using Electrons on Liquid Helium for Quantum Computing

A.J. Dahm^a, J.M. Goodkind^b, I. Karakurt^a, and S. Pilla^b

^a*Department of Physics, Case Western Reserve University, Cleveland, OH 44106-7079, USA*

^b*Department of Physics, University of California at San Diego, La Jolla, CA 92093-0319, USA*

(November 4, 2001)

We describe a quantum computer based on electrons supported by a helium film and localized laterally by small electrodes just under the helium surface. Each qubit is made of combinations of the ground and first excited state of an electron trapped in the image potential well at the surface. Mechanisms for preparing the initial state of the qubit, operations with the qubits, and a proposed readout are described. This system is, in principle, capable of 10^5 operations in a decoherence time.

PACS numbers: 03.67.Lx, 73.20.-r.

I. INTRODUCTION

A full description of quantum computing is beyond the scope of this paper. More complete descriptions are given elsewhere.¹

A classical computer has binary bits with values that are either 0 or 1. A quantum computer is operated with quantum bits, called qubits. Each qubit uses two energy levels of a quantum system for the components 0 and 1. However, a qubit can be in a state that is a superposition of these two components,

$$\Psi = a|0\rangle + b|1\rangle; \quad |a|^2 + |b|^2 = 1 \quad (1)$$

A quantum computer would use a superposition of many qubit states. An n -qubit system has 2^n basis vectors, $|x_j\rangle$, which can be taken as products of the basis vectors of each of the n qubits. An arbitrary combination of these can be written as

$$\Psi = \sum_j \alpha_j |x_j\rangle; \quad \sum_j |\alpha_j|^2 = 1 \quad (2)$$

An example of a basis vector for the five qubit case (for $j = k$) is, $|x_k\rangle = |01100\rangle$.

The superposition states represented by Eqs. (1) and (2) are responsible for the great potential advantage of quantum logic operations relative to classical ones. In the classical case an operation starts, proceeds and ends with every qubit in a given state. In the quantum case, an operation can use qubits in a superposition of many possible basis states. Operation on such superposition states can be equivalent to performing a large number of computations in parallel. The difficulty in utilizing this advantage arises from the fundamental nature of measurement in quantum processes, namely that measurement of the energy of an individual qubit will necessarily collapse the wave function so that the result can be only either $|0\rangle$ or $|1\rangle$ for each qubit. This requires algorithms that can yield definite answers to computations even though the square of the coefficients α_j represent only probabilities.

For quantum logic operations with a physical system one must have

- a) discrete states that can be identified with the components $|0\rangle$ or $|1\rangle$.
- b) a method to prepare an initial state.
- c) a method for operating quantum gates.
- d) a readout mechanism.
- e) a coherence time sufficient to undertake a large number of operations.
- f) for practical computing the system must be scalable to a large number of qubits.

We describe here a proposed quantum computer with qubits made of electrons on the surface of a liquid helium film and describe our method for fabricating the qubits and the methods by which their quantum states can be manipulated and measured. This system was first proposed by Platzman and Dykman² and has been described elsewhere.³⁻⁶

II. ELECTRONS ON HELIUM

Electrons are bound to the surface of liquid helium by the dielectric image potential. A repulsive Pauli potential prevents them from penetrating into liquid helium. The hydrogenic-like potential is of the form

$$V = -\Lambda e^2/z; \quad \Lambda = (\kappa - 1)/4(\kappa + 1), \quad (3)$$

where z is the coordinate normal to the surface, and κ is the dielectric constant of helium. The energy levels form a Rydberg spectrum, $E_n = -R/n^2$. We give parameters for liquid ³He; $\Lambda_3 = 0.00521$, $R_3 = 0.37$ meV, and the Bohr radius for this problem is $a_B = 10.2$ nm. The average separation of the electron from the surface is $\langle z \rangle = 15.3$ nm and 61 nm for the ground and first excited state, respectively. The transition frequency between the ground and first excited state⁷ is 70 GHz. These transitions can be shifted with a Stark field⁸ applied normal to the surface. The potentials with and without a Stark field are shown in Fig. 1.

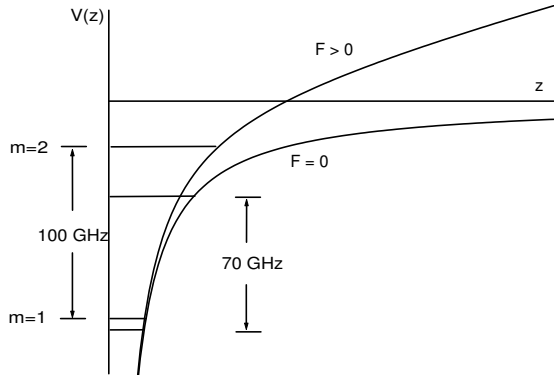


FIG. 1. The potentials and energy levels with and without an electric field F applied normal to the surface. The ground ($m=1$) and first excited ($m=2$) energy levels for each potential are indicated schematically.

III. DESIGN OF THE COMPUTER

We identify the ground and first excited states of these electrons with the states $|0\rangle$ and $|1\rangle$, respectively. In order to address and control the qubits each electron must be localized laterally. This will be accomplished by locating electrons above microelectrodes (posts) that are separated by about $0.5 \mu\text{m}$. The electrons will be separated from the tops of the posts by a $0.5 \mu\text{m}$ thick helium film. The lateral confinement results from the image potentials of the posts and the electric field from the potential on the posts, and the electron will be in the ground state for lateral motion at low temperatures.

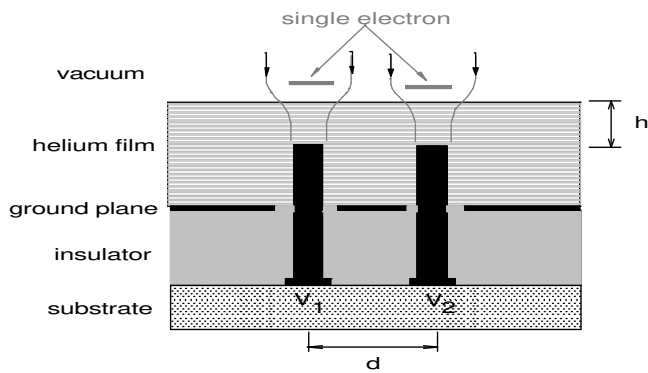


FIG. 2. The geometry of a two-qubit system with electrons above the microstructure and the helium film. Electric field lines are shown. Drawing is not to scale. The optimal dimensions are $d \approx h = 0.5 \mu\text{m}$. Control potentials V_1 and V_2 are applied on the micro-electrodes.

A schematic of posts and electrons for a two-qubit system is shown in Fig. 2. A voltage applied to a given post controls the Stark field for the corresponding electron. An array of posts fabricated at the Cornell Nanofabrica-

tion Facility is shown in Fig. 3. A prototype with lead wires to the posts and an isolated ground plane to screen the field from the leads has also been fabricated. Numerical computations of the electric field from the posts and ground plane have been completed and fabrication of a final design is in progress. Note that this system is scalable to an arbitrary number of posts or qubits.

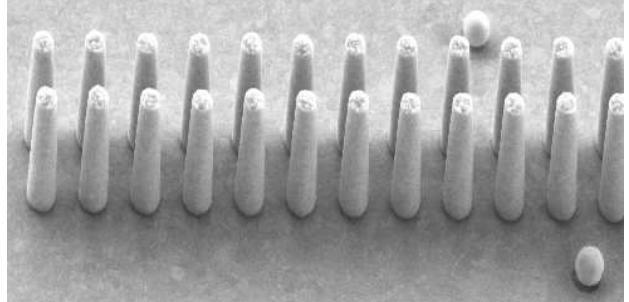


FIG. 3. SEM image of double row of posts grown on a gold film. The posts are $1.5 \mu\text{m}$ high and separated by $0.5 \mu\text{m}$.

A schematic of our cell is shown in Fig. 4. The posts will be located in the bottom of a waveguide that transmits sub-mm radiation to the electrons. Superconducting microbolometers will be located at the top of the guide to detect electrons that are allowed to escape from the posts. A tunnel-diode electron-emission source will be located above the electron detectors. Electrons will be loaded onto the film through a hole in the detector chip, and one electron will be trapped over each post by an applied positive potential. The thickness of the helium film will be measured with a capacitor made of metal strips deposited on a part of the ground plane containing the posts that extends outside of the waveguide. The electrodes of the capacitor are in the shape of a comb with interwoven teeth spaced by approximately one micron. The system will be operated at 10 mK to increase coherence times of the qubit states.

Our initial tests will be on a ^3He film. The microwave setup for ^3He is easier to work with because the transition frequencies are lower and the corresponding waveguide is larger. There are a number of other advantages in using ^3He . Liquid ^3He has a large viscosity at low temperatures. This should severely dampen high-frequency ripplons involved in T_1 and T_2 processes, although new decoherence processes involving interactions with the bulk ^3He may occur. Thermal contact between the sample chamber and ^3He is much easier to achieve than for ^4He , and the surface is less affected by microphonics. Finally, the larger separation of the electrons from the surface leads to a somewhat larger dipole interaction between neighboring states.

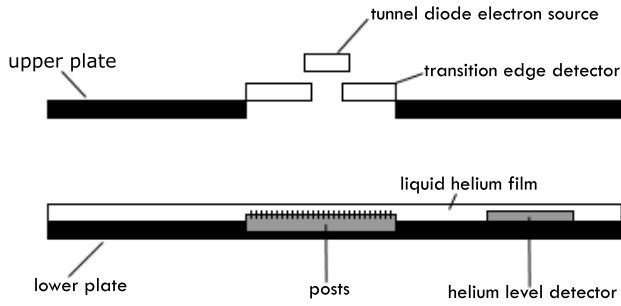


FIG. 4. Schematic of the cell. The upper plate includes detectors used in the readout. The lower plate includes the posts and is covered with the helium film. The electrons float over the posts about 10 nm above the surface of the helium film.

IV. OPERATIONS

The operation would normally begin with all qubits in the ground state. Then according to the requirements of the desired operations, each qubit would be prepared in some admixture of states $|0\rangle$ and $|1\rangle$ by Stark shifting individual qubits into resonance with microwave radiation for a predetermined time.^{3,5} The state of the qubit n will be

$$\Psi_n = \cos(\Theta_n/2)|0\rangle - i \sin(\Theta_n/2)|1\rangle, \quad (4)$$

where $\Theta_n = \Omega\tau_n$, $\Omega = eE_{rf}\langle 1|z|2\rangle/\hbar$ is the Rabi frequency, E_{rf} is the strength of the rf field, and τ_n is the time the n^{th} qubit is in resonance with the microwave field.

In general, computations will be implemented by applying pulses of radiation to interacting qubits. We illustrate a potential operating mode of the system by describing two qubits operated as a swap gate. The interaction between qubits is via the Coulomb energy, which is much larger than the interaction between the induced dipole moment of each qubit. The dipolar component of the direct interaction potential between qubits i and j is

$$V(z_i, z_j) \sim (e^2/8\pi\epsilon_0 d^3)(z_i - z_j)^2, \quad (5)$$

where d is the electron separation, and z_i is the separation of the i^{th} electron from the helium surface. Start with one qubit in the state $|0\rangle$ and the other in the state $|1\rangle$. Next apply the same Stark fields to both qubits so that the states $|01\rangle$ and $|10\rangle$ would be degenerate. In this condition the system will oscillate between the two states at a frequency given by the interaction energy, which in first order is given by $\sim e^2 a_B^2/4\pi\epsilon_0 d^3$. This frequency is ~ 1 GHz for a separation of $0.5 \mu\text{m}$. By leaving the electric fields in this condition for one half cycle of this oscillation, the two qubits will swap states. It will be difficult to tune neighboring qubits to precisely identical Stark shifts, and in practice we may sweep the Stark

shift of one qubit through resonance with a neighboring qubit.⁵ In this case, the final state of the qubit will depend on the rate at which the electric field is swept through the resonance condition.

Readout. The wavefunction of the system of entangled qubits collapses when a measurement is made. Thus, the states of all qubits must be read within the time scale is set by the plasma frequency ~ 100 GHz. We describe here our initial proposal for a destructive readout pending research into other schemes. We will apply a short, ~ 1 ns, ramp of an extracting electric field to all qubits. The potential for a fixed value of extracting field is shown in Fig. 5. The tunneling probability is exponential in the time-dependent barrier height. All electrons in the upper $|1\rangle$ state will tunnel through the barrier within a short period of time when this probability becomes sufficiently large. The escape of an electron will be detected by the bolometer detector mentioned above. For this extracting field the tunneling probability will be negligibly small for electrons in the ground $|0\rangle$ state. After the ramp is removed the remaining electrons will be in the ground state. Subsequently, we plan to sequentially apply to each post an extracting field sufficiently large so that electrons in the ground state will tunnel from the surface.⁹ A $|0\rangle$ will be registered for each electron detected and a $|1\rangle$ for those states that are empty.

An alternate scheme would be to apply an extracting voltage to the post under one electron at a time. For small numbers of qubits in our initial exploratory experiments, the system would then be prepared in the same state repeatedly and a different qubit sampled each time the operation is carried out. Ultimately we hope to develop a non-destructive readout that will allow simultaneous measurement of the states of all qubits without allowing the electrons to escape.

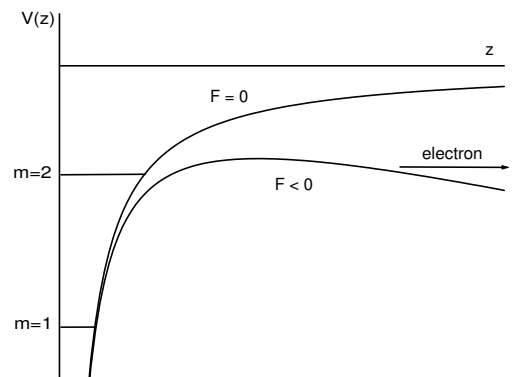


FIG. 5. The potential with an extracting field.

V. DECOHERENCE

All logic operations must be accomplished in less time than it takes for the interactions of the qubit with the environment to destroy the phase coherence of the state

functions. For electrons on ^4He the lifetime of the excited state $|1\rangle$ is limited by interactions with riplons. The electron-riplon coupling Hamiltonian^{2,3,5} is

$$H_{er} = eE_{\perp}\delta, \quad (6)$$

where E_{\perp} is the normal component of the electric field that includes both the applied field and variations in the helium dielectric image field due to surface distortions, and δ is the amplitude of the surface height variation. The average rms thermal fluctuation of the surface is

$$\delta_T = (k_B T / \sigma)^{1/2} \cong 2 \times 10^{-9} \text{ cm} \quad (7)$$

The transition from the excited to ground state requires a ripplon with a wave vector $\cong a_B^{-1}$. For a single electron on bulk helium a radiationless transition occurs with the energy absorbed by electron plane-wave states for motion parallel to the surface and momentum absorbed by riplons. For this case a calculation of T_1 yields

$$T_1^{-1} \cong \Delta\nu(\delta_T/a_B)^2, \quad (8)$$

where $\Delta\nu$ is the transition frequency. At $T = 10$ mK, $\delta_T/a_B \cong 10^{-3}$, and $T_1 \cong 10\mu\text{s}$.

For electrons confined by posts, the lateral states are harmonic oscillator states of the image potential well of the posts. These are separated in energy¹⁰ by $\hbar\Omega_1 \approx \hbar(e^2/4\pi\epsilon_0 m d^3)^{1/2} \sim 300$ mK. For an array of electrons there is a band of plasma oscillations associated with each harmonic oscillator level, which for an electron separation of $0.5\mu\text{m}$ on bulk helium has a band width that is greater than 300 mK. The confining potential of the posts reduces the width of this band. Preliminary calculations¹⁰ suggest that the width may be sufficiently small to prevent conservation of energy in a radiationless transition. This is illustrated in Fig. 6 where the transition is shown to be incommensurate in energy with an excitation between the harmonic oscillator states. Suppression of this relaxation channel would lead to a very large value of T_1 .

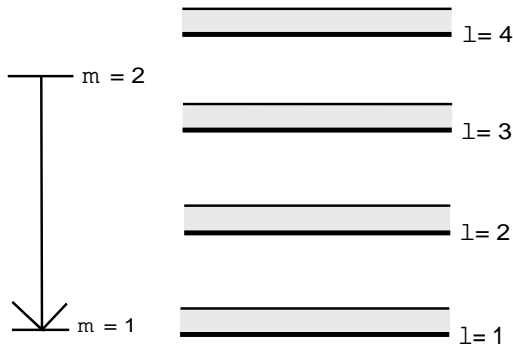


FIG. 6. Energy level schematic. The integer m labels the hydrogenic-like states, and the integer l labels lateral states, which are harmonic oscillator states in the image field of the posts or Landau levels in a magnetic field. The hatched region indicates the band of plasma oscillations associated with each level.

If the confining potential does not sufficiently reduce the width of the plasma band, this will be accomplished with an applied magnetic field. A magnetic field confines the lateral states to Landau levels with a band of plasma oscillations of width $\hbar\Omega_2 \sim \hbar\omega_p^2/\omega_c$. Here ω_p and ω_c are, respectively, the zone-boundary plasmon of the ordered qubit array and cyclotron frequencies. The transitions between Landau levels with the emission of one ripplon cannot conserve energy and momentum for $B \cong 1.5$ Tesla.

The two-riplon process can either cause a transition to the ground state or lead to dephasing by an incoherent phase modulation due to quasi-elastic scattering within a "hydrogenic level" by thermal riplons with a wave vector equal to the inverse cyclotron radius¹¹. At 10 mK and a field of 1.5 Tesla, this leads to a dephasing time¹⁰ T_2 of ~ 100 ms. Single operations can be made in 1 ns. Thus, in principle, $\sim 10^5$ operations can be performed in a decoherence time.

High frequency riplons are strongly damped on a liquid ^3He surface. Thus, it is possible that the values of T_1 and T_2 may be longer than for ^4He . A possible dephasing mechanism for the case of ^3He is via interactions of the electron with excitations on the Fermi surface of bulk ^3He . Theoretical calculations of this mechanism have not been carried out.

ACKNOWLEDGMENTS

The authors wish to acknowledge Mark Dykman for helpful conversations. This work was supported in part by NSF grant EIS-0085922.

¹ See for example, M.A. Nielsen and I.L. Chuang, *Quantum Computation and Quantum Information* (Cambridge University Press, Cambridge, 2000), or H-K. Lo, S. Popescu, and T. Spiller, *Introduction to Quantum Computation and Information* (World Scientific, Singapore, 1998).

² P.M. Platzman and M.I. Dykman, *Science* **284**, 1967 (1999).

³ M.I. Dykman and P.M. Platzman, *Fortschr. Phys.* **48**, 1095 (2000).

⁴ M.J. Lea, P.G. Frayne, and Yu. Mukharshy, *Fortschr. Phys.* **48**, 1109 (2000).

⁵ M.I. Dykman and P.M. Platzman, *Quantum Information and Computation* **1**, to be published.

⁶ J.M. Goodkind and S. Pilla, *Quantum Information and Computation* **1**, to be published.

⁷ A.P. Volodin and V.S. Edel'man, *Zh. Eksp. Teor. Fiz.* **81**, 368 (1981); *JETP* **54**, 198 (1981).

⁸ C.C. Grimes and G.A. Adams, *Phys. Rev. Lett.* **42**, 795 (1979).

⁹ G.F. Saville and J.M. Goodkind, *Phys. Rev. A.* **50**, 2059 (1994).

¹⁰ M.I. Dykman and P.M. Platzman, to be published.

¹¹ M.I. Dykman, *Phys. Status Solidi B* **88**, 463 (1978).